J Solid State Electrochem (2011) 15:1077–1085
DOI 10.1007/s10008-010-1166-x

ORIGINAL PAPER

Chlorine contaminants poisoning of solid oxide fuel cells

Ting Shuai Li · Cheng Xu · Tao Chen · He Miao · Wei Guo Wang

Received: 17 May 2010 / Accepted: 2 August 2010 / Published online: 19 August 2010

Abstract Investigation has been conducted on the poisoning effect of various contaminants containing chlorine at ppm level (<10 ppm) on the performance of Ni-YSZ anode-supported solid oxide fuel cells. The results indicate that cell performance drops by exposure to 1 ppm Cl_2(g) at 750 °C, whereas the introduction of Cl_2(g) with concentration higher than 5 ppm causes only a slight degradation at 850 °C. The presence of 2–6 ppm CH_3Cl(g) and C_2H_3Cl(g) can also induce measurable cell performance decline at 750 and 850 °C and this deterioration cannot be completely removed after switching to pure fuel at 850 °C. No performance loss is found when the cell is operated in fuel containing 1–8 ppm HCl(g) at 750 and 850 °C. It is thus concluded that chlorine in the form of Cl_2(g) yields the largest poisoning effect at 750 °C, while the degradation rate caused by addition of C_2H_3Cl(g) increases with the increase of operation temperature. Agglomerations at anodic region are observed in the samples after poisoning test by Cl_2(g), CH_3Cl(g), and C_2H_3Cl(g), but the anode microstructure is uniform for the sample exposed to HCl(g) for poisoning test.

Keywords Solid oxide fuel cells · Chlorine · Degradation · Recover · Microstructure

Introduction

Coal is currently believed to be the most economical fuel and possesses a great potential for clean power generation along with the development of gasification technology [1]. Raw coal syngas directly derived from gasification system has compositions varying significantly with the rank and the origin of the coal and thereafter specific gasification processes [2, 3]. Four major compounds including CO, H_2, CO_2 and H_2O usually account for more than 90% of the content in the coal syngas. Other syngas compositions include traces of impurities such as S, Cl, P, As, et al. which cannot be completely removed in gasification processes [4].

Solid oxide fuel cell (SOFC) is a promising candidate for clean power generation due to its high efficiency and no emission. Most importantly, the capability of SOFC operating under diverse fuels enhances its potential for clean energy industry applications. Although there are great advantages for coal syngas to be used in SOFC system, various contaminants in syngas have detrimental effects on SOFC cermet anode and thus induce cell performance degradation. Among these contaminants, hydrogen sulfide has been widely studied [5–7], but more attention should be paid on the effect of various contaminants containing chlorine because of their stable presence in coal syngas and tangible poisoning effect on SOFC.

Chlorine contaminants in coal-derived syngas usually exist in the forms of Cl_2(g), CH_3Cl(g) and HCl(g). Several reports have shown that the performance of SOFC single cell deteriorates by exposure to chlorine contaminants at ppm level. Trembly et al. [8] reported cell performance loss in an electrolyte-supported button cell with 17.4% and 13.3% decreases in current density by exposure to 20 ppm HCl in the syngas fuel at 800 and 900 °C, respectively. Haga et al. also observed sluggish degradation in cell voltage using an electrolyte-supported button cell when fueled with hydrogen containing 5 ppm Cl_2(g) at 800 °C [9]. Krishnan et al. [4] found no measurable degradation by exposure to 40 ppm CH_3Cl(g) for 140 h at 800 °C, but observed increasing degradation rate with time at 850 °C.

T. S. Li · C. Xu · T. Chen · H. Miao · W. G. Wang (✉)
Division of Fuel Cell and Energy Technology,
Ningbo Institute of Material Technology and Engineering,
Chinese Academy of Sciences,
519 Zhuangshi Road,
Ningbo 315201, China
e-mail: wgwang@nimte.ac.cn

CH_3Cl(g) and HCl(g) are two important forms of chlorine in coal syngas [3] and most of investigations on chlorine poisoning have been conducted using fuel containing CH_3Cl(g) or HCl(g). Bao et al. [10] investigated a typical Ni-YSZ anode-supported cell and found no significant degradation by exposure to 40 ppm HCl(g) for 100 h at 750 and 800 °C, neither did the cell degrade by exposure to 40 ppm of CH_3Cl(g) at 800 °C. Notable degradation in cell performance was only detected after ~80 h exposure to 40 ppm of CH_3Cl(g) at 850 °C. This insensitivity of cell performance to chlorine contaminants at ppm level is very different from the results in [8], suggesting the anode-supported cell in [10] seems more tolerant to HCl poisoning than the electrolyte-supported cell in [8]. Therefore, cell fabrication may affect the poisoning behavior caused by various chlorine contaminants in coal-derived gas.

In order to understand chlorine poisoning behavior, several mechanisms have been proposed. Most of them are focused on HCl poisoning behavior and some of them have discussed about CH_3Cl poisoning. Trembly et al. [8] suggested the reaction between Ni and HCl(g) to form chloride $NiCl_2$, accounting for degradation caused due to addition of HCl(g) contaminant. Haga et al. [9] attributed HCl(g) poisoning behavior to microstructural change and a lower nickel-to-zirconia ratio due to the formation of $NiCl_2$. Krishnan et al. [4] attributed the visible CH_3Cl poisoning to the adsorption of Cl atom on the surface of Ni catalyst. Bao et al. [11] argued the CH_3Cl(g) poisoning was due to the decomposition resultants of CH_4(g) and HCl(g) under SOFC operating conditions. However, the soundness of this mechanism is debatable since 2.5 ppm CH_3Cl(g) can only produce 2.5 ppm HCl(g) according to the decomposition reaction, but no cell performance degradation had been detected in the cell exposed to 40 ppm HCl(g) [10]. Besides the above mechanisms, it was reported recently that chlorine contained impurity can migrate poisoning effect caused by other forms of contaminants containing As and P element [12]. More experimental results and discussion are required to validate this mechanism.

It has been shown that Cl-related contaminants in coal syngas (after Rectisol cleanup) consist of 2 ppm CH_3Cl and less than 1 ppm HCl [4]. It is thus imperative to investigate the poisoning behavior caused by chlorine contaminants at ppm level in fuel gas so as to achieve poisoning control. A number of investigations have been conducted in the poisoning effect of chlorine on SOFCs, but there are still some discrepancies in understanding of the poisoning behavior of chlorine contaminants (Cl_2(g), HCl(g), CH_3Cl (g) and C_2H_3Cl(g)) under SOFC operating conditions, such as poisoning mechanisms, the temperature dependence of poisoning extent and morphology changes due to the introduction of contaminants. In this study, the dependence of degradation behavior on forms of chlorine contaminants at practical ppm level (<10 ppm) is investigated under various cell operating conditions. Poisoning effects of four major Cl-related contaminants, Cl_2(g), HCl(g), CH_3Cl(g), and C_2H_3Cl(g), are compared with propose the dominating poisoning mechanism. The poisoning mechanisms are also discussed to evaluate the possibility of poisoning control in practical applications.

Experimental

Commercial Ni-YSZ anode-supported SOFCs were received from Ningbo Institute of Material Technology and Engineering (NIMTE), Chinese Academy of Sciences. The cells had a 10×10 cm dimension and consisted of a double cathode layer including a strontium-doped lanthanum manganite perovskite (LSM) current collector layer of about 30 μm thick and a LSM-YSZ functional layer of 25~30 μm thick, a yttria-stabilized zirconia (YSZ) electrolyte layer of 10 μm thick, a Ni-YSZ active layer of 10 μm thick and a Ni-YSZ supporting layer of approximately 400 μm thick. The cells were cut into samples of 5×5.8 cm^2 with an active area of 4×4 cm^2 and then tested in alumina testing houses confined between gas-distributor plates made of nickel foam at the anode side and LSM sandwiched by silver mesh at the cathode side. The resistance of these plates can be negligible due to a four-wire testing configuration. Details on the testing facility had been described elsewhere [13].

The cells were heated up to 850 °C at a rate of 1 °C min^{-1} and were kept at 850 °C for 3 h with hydrogen of 300 Nml min^{-1} at the anode side and air at the cathode side with a flow rate of 500 Nml min^{-1} to achieve complete reduction of NiO to Ni [14]. After reduction, the cells were operated galvanostatically at 0.25 A cm^{-2} for at least 10 h to avoid sharp electrode activation [15]. All poisoning tests were conducted at 750 and 850 °C with 2,000 Nmlmin^{-1} of air as cathode gas flow and 800 Nml min^{-1} of hydrogen containing a few ppm contaminants including Cl_2(g), HCl(g), CH_3Cl(g), and C_2H_3Cl(g) at the anode side. All the contaminants were added separately into the fuel through a mass flow meter with concentrations ranging from 1 to 8 ppm at a concentration increase rate of 1 ppm per hour.

The cell performance was evaluated by measuring real-time current–voltage (*I–V*) curves at 750 and 850 °C. Electrochemical impedance spectra (EIS) were recorded using an Electrochemical Workstation (IM6ex ZAHNER) with a scanning frequency range from 2 MHz to 0.05 Hz at open circuit voltage. Microstructural analysis was conducted on the as-tested cells using a Hitachi S4800 Field Emission Scanning Electron Microscope (FE-SEM/EDS).

Results and discussion

Figure 1 shows *I–V* (current density versus cell voltage) curves for a typical SOFC single cell used for investigation. The cell performance is obtained after more than 10 h activation and represents a moderate performance level of the cells manufactured at NIMTE. The cell exhibits an open circuit voltage of 1.115 V at 750 °C and 1.104 V at 850 °C while the maximum power density is 0.4 W cm^{-2} at 750 °C and 0.6 W cm^{-2} at 850 °C. It has been shown that the cells in NIMTE can be stably operated at temperatures ranging from 700 to 850 °C using pure hydrogen as fuel for approximately 1,000 h without conspicuous degradation [16].

Figure 2a shows the variation of cell voltage with time by exposure to 1–4 ppm Cl_2(g) at 850 °C. Each 1 ppm Cl_2(g) change has remained for 3 h to obtain stabilized poisoning effects. As shown in Fig. 2a, no measurable degradation in cell performance can be detected through the whole process. However, the performance deterioration becomes slightly legible when the concentration of Cl_2(g) increases to higher than 5 ppm as displayed in Fig. 2b. A continuous degradation trend can also be inspected and a constant degradation rate of 0.24%h^{-1} (ppm^{-1}) is obtained for different ppm levels, suggesting a Cl_2(g) concentration of less than 10 ppm may not drastically aggravate the poisoning effect at 850 °C. On the opposite, the poisoning effect may be slowed down with the increase of Cl_2(g) concentration since the fuel adjustment for higher ppm level induces fuel flow reduction which may magnify the poisoning extent.

Figure 3a exhibits the variation of cell voltage with time when the cell is exposed to 1–4 ppm Cl_2(g) at 750 °C. The poisoning extent, calculated from the ratio of voltage decrease to initial voltage, increases from 1.5% to 2.8% of the initial voltage of 844 mV with increasing Cl_2(g) concentration from 1 to 4 ppm. This performance drop observed at 750 °C is much larger than the degradation effect at 850 °C, indicating the decease of operation temperature can aggravate poisoning effect. The content of Cl_2(g) in fuel is then increased to 5 and 6 ppm as shown in Fig. 3b to inspect the dependence of poisoning extent on Cl_2(g) content. The degradation in cell performance by exposure to 5 ppm Cl_2(g) is almost the same as the degradation by exposure to 4 ppm Cl_2(g), but the degradation increases to 3.0% when Cl_2(g) content reaches 6 ppm. All degradations shown in Fig. 3 can be completely recovered within 45 min after switching to Cl_2(g)-free fuel gas atmosphere.

The effect of HCl(g) of 1–10 ppm on the cell performance is shown in Fig. 4. No significant degradation is observed during the test even by increasing the HCl(g) concentration up to 8 ppm at 850 °C and 10 ppm at 750 °C. It has been reported that the chlorine contaminant in the form of HCl(g) in coal gas (after Rectisol cleanup) is less than 1 ppm [4], therefore it can be concluded that the effect of HCl in coal-derived syngas on cell performance can be neglected at least

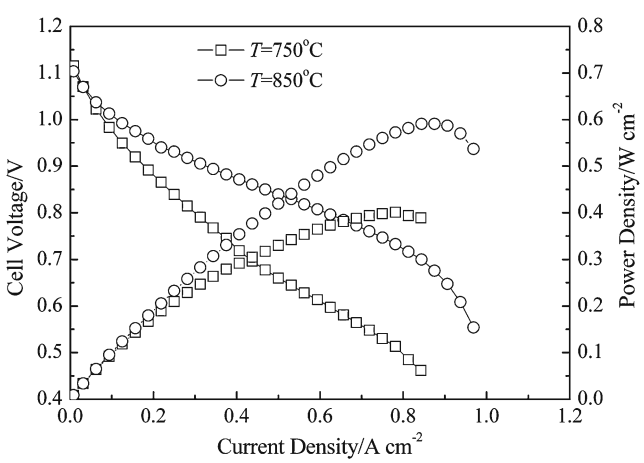

Fig. 1 Electrochemical performance for a typical anode-supported SOFC single cell

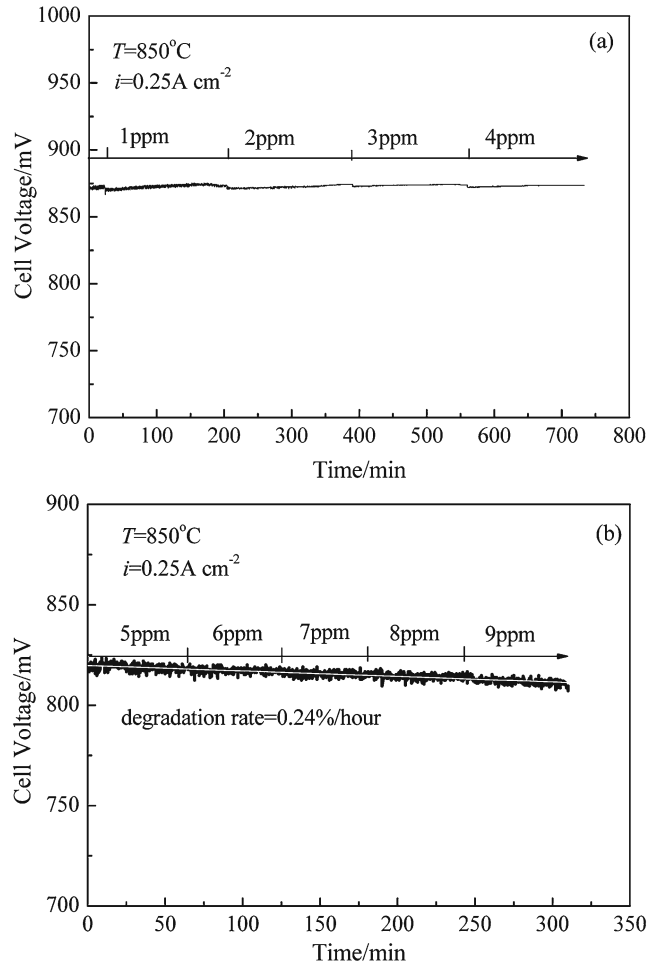

Fig. 2 Variation of cell voltage for the cells subjected to poisoning tests at 850 °C with Cl_2 concentration: **a** at 1~4 ppm level; **b** at 5~9 ppm

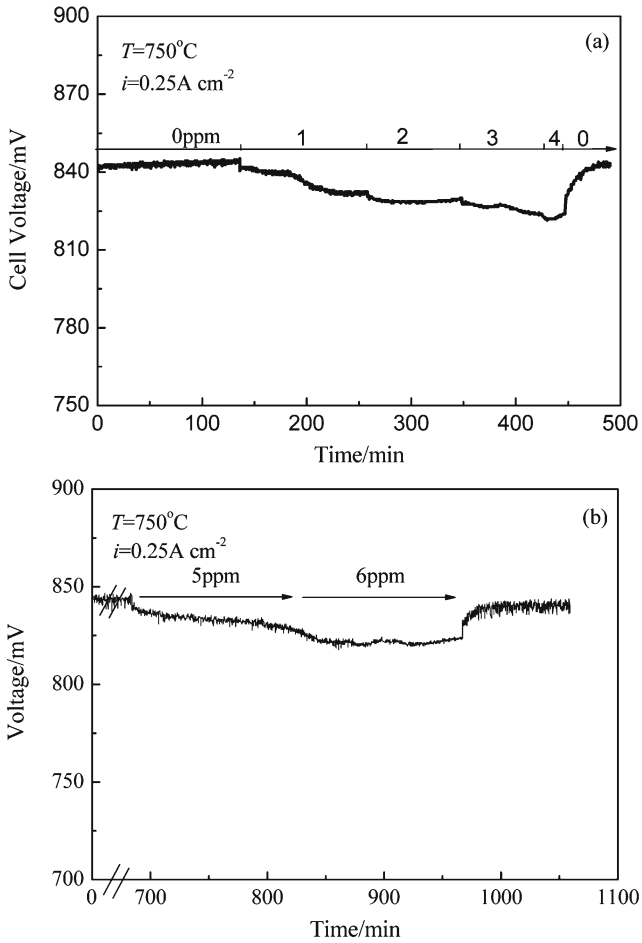

Fig. 3 Variation of cell voltage for the cells subjected to poisoning tests at 750 °C with Cl_2 concentration: **a** at 1~4 ppm level; **b** at 5~6 ppm

when the cell is fueled with practical coal-derived syngas at temperatures ranging from 750 to 850 °C. The cell voltage variation induced by exposure to 2–6 ppm CH_3Cl(g) in fuel for the cell operated at 750 °C is shown in Fig. 5a.

The CH_3Cl(g) of 2 and 6 ppm incurs performance drops of 1.6% and 2.8% of the initial voltage value of 834 mV, respectively. These deterioration can be rapidly recovered within 25 min after switching off the CH_3Cl(g) flow. It is noted that no severe degradation is detected when the concentration increases from 2 to 4 ppm. This is similar to the degradation effect of 5 ppm Cl_2(g) as shown in Fig. 4b, indicating the poisoning effect of Cl-containing contaminants may not increase in proportion with the contaminant concentration.

Figure 5b shows the variation of cell voltage with time by exposure to 2–6 ppm CH_3Cl(g) at 850 °C. The effect of CH_3Cl(g) on cell performance is reduced by increasing operation temperature from 750 to 850 °C. The poisoning extent increases from 0.45% to 1.1% of 883 mV with the increase of CH_3Cl(g) content from 2 to 6 ppm. The degradation in cell performance cell by exposure to 4 ppm and 6 ppm CH_3Cl(g) cannot be completely removed

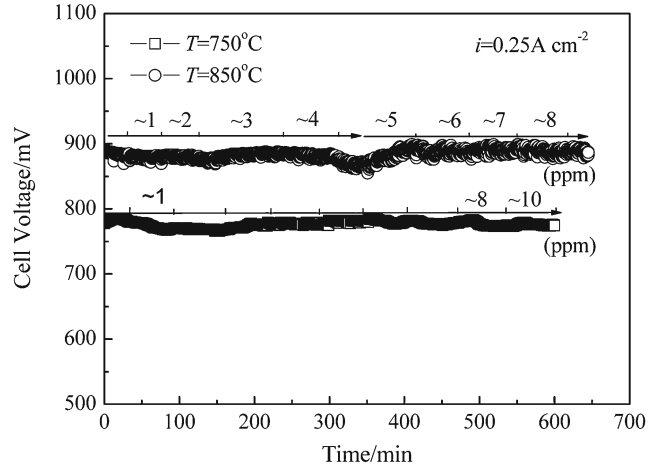

Fig. 4 Variation of cell voltage for the cells subjected to poisoning tests at 750 and 850 °C with different HCl concentration

through regeneration: 99% of cell voltage can be regenerated after removal of the contaminant.

Figure 6a shows the variation of cell voltage caused by the addition of 2–6 ppm C_2H_3Cl(g) to fuel gas for the cell

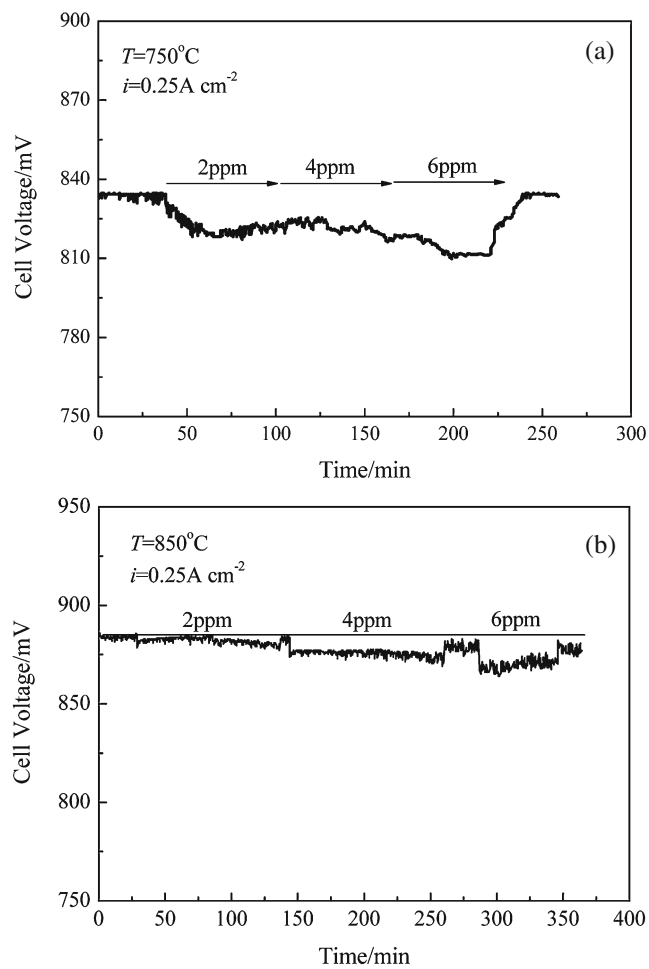

Fig. 5 Variation of cell performance caused by CH_3Cl injection: **a** at 750 °C; **b** at 850 °C

tested at 750 °C. When the C_2H_3Cl concentration increases from 2 to 6 ppm, the degradation degree increases from 0.23% to 1.3% of the initial voltage value of 865 mV. This deterioration extent can be fully recovered by stopping C_2H_3Cl injection. For the cell tested at 850 °C, although the performance drop is identically on the rise from 0.86% to 1.5% of 932 mV with the increase of C_2H_3Cl(g) concentration (Fig. 6b), the voltage can be eventually recovered to 99% of the original voltage value (932 mV). It also shows that as the temperature increases from 750 to 850 °C, the degradation rate caused by the same ppm level slightly increases. The temperature dependence of C_2H_3Cl poisoning effect is opposite to the results for poisoning by Cl_2 and CH_3Cl. The latter causes increasing poisoning extent with the decreasing operation temperature.

The effect of coal syngas impurities containing chlorine on the performance of solid oxide fuel cells is summarized in Fig. 7a for the cell operated at 750 °C and Fig. 7b for the cell operated at 850 °C. It can be seen that Cl_2(g) results in the largest performance drop at 750 °C if the four forms of contaminants containing chlorine are at the same level. The performance degradation generated by CH_3Cl(g) contaminant is a bit less than that of Cl_2(g) and the poisoning effect induced by the C_2H_3Cl(g) is much weaker. No noticeable deterioration is observed after introducing HCl(g) into fuel gas. However, the poisoning effect for the four contaminants varies when testing at 850 °C under identical conditions. It can be seen in Fig. 7b that poisoning degree aroused by C_2H_3Cl(g) is the highest at 850 °C while CH_3Cl (g) takes the second place and Cl_2(g) the third. No visible degradation is found for the addition of HCl(g).

The above results can be further verified by EIS as displayed in Fig. 8 for the cell tested at 750 °C. The polarization resistance (*Rp*) corresponding to frequency ranges below 10 Hz apparently increases with the increase of Cl_2(g) concentration as shown in Fig. 8a. Nevertheless, no measureable deviation in these recorded spectra as the concentration of HCl(g), CH_3Cl(g), and C_2H_3Cl(g) increases as displayed in Fig. 8b–d. This may be due to the slight variation incurred by these forms of chlorine is difficult to be captured using the EIS technique. The frequency ranges exhibiting the polarization increase with Cl_2(g) concentration increase have been reported to correspond to diffusion and gas conversion processes at the anode [17, 18]. It thus suggests the addition of Cl_2(g) to fuel can increase the difficulty in gas diffusion and gas conversion at anode chamber at 750 °C. To be noted that the series resistance (*Rs*) shows no deviation after the injection of all the four contaminants. The *Rs* has been defined as electrode resistance and interfacial resistance between electrode and electrolyte [19]. Therefore, the effect of contaminants containing Cl on the interface microstructure between the anode and the electrolyte and the anode microstructure is limited. This is partially due to the tiny amount of contaminants.

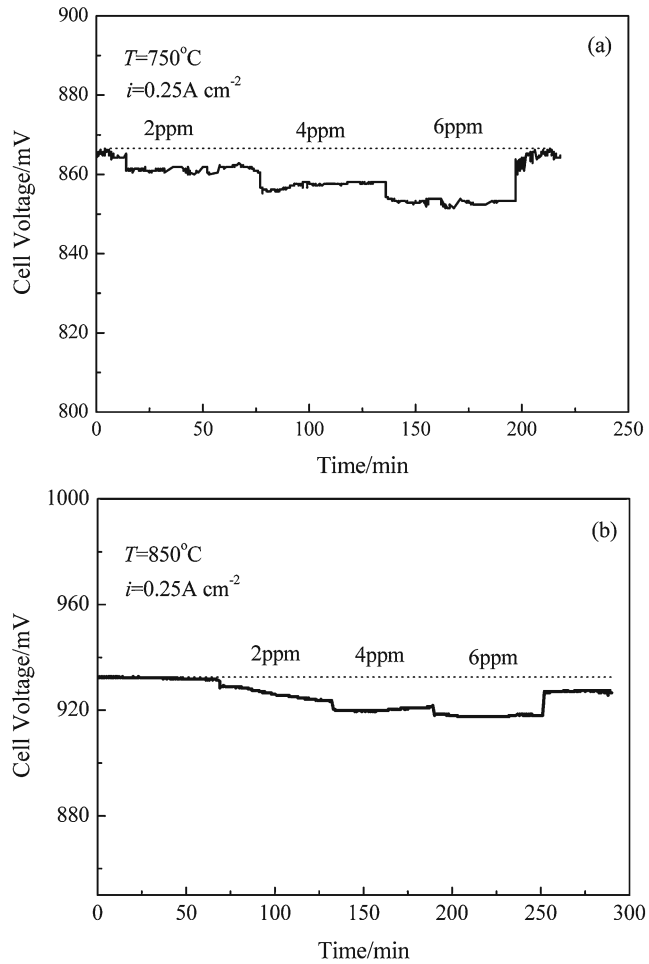

Fig. 6 Variation of cell performance caused by C_2H_3Cl introduction: **a** at 750 °C; **b** at 850 °C

Figure 9 displays EIS results for the cell fueled with hydrogen containing CH_3Cl(g) and C_2H_3Cl(g) at 850 °C. A significant increase in polarization resistance is observed for the cell upon exposure to both CH_3Cl(g) and C_2H_3Cl(g). When the C_2H_3Cl(g) content increases from 2 to 6 ppm in fuel, the *Rp* accordingly increases from 1.65 Ωcm^{-2} to 2.78 Ωcm^{-2} and the *Rp* value for the cell exposed to CH_3Cl (g) goes up from 0.94 Ωcm^{-2} to 1.55 Ωcm^{-2} with CH_3Cl(g) concentration rising from 2 to 4 ppm. These increases are much larger than the cell exposed to the same contaminants at 750 °C, indicating the increase of operation temperature aggravates the poisoning effect. Also, it is observed that the increase of *Rp* mainly occurs at the second arc of the EIS where the frequency range is below 10 Hz. This frequency ranges has been reported to involve diffusion and gas conversion processes, suggesting the addition of CH_3Cl(g) and C_2H_3Cl(g) to fuel at 850 °C can detrimentally affect hydrogen diffusion to anode active layer and conversion to water and result in cell performance drop.

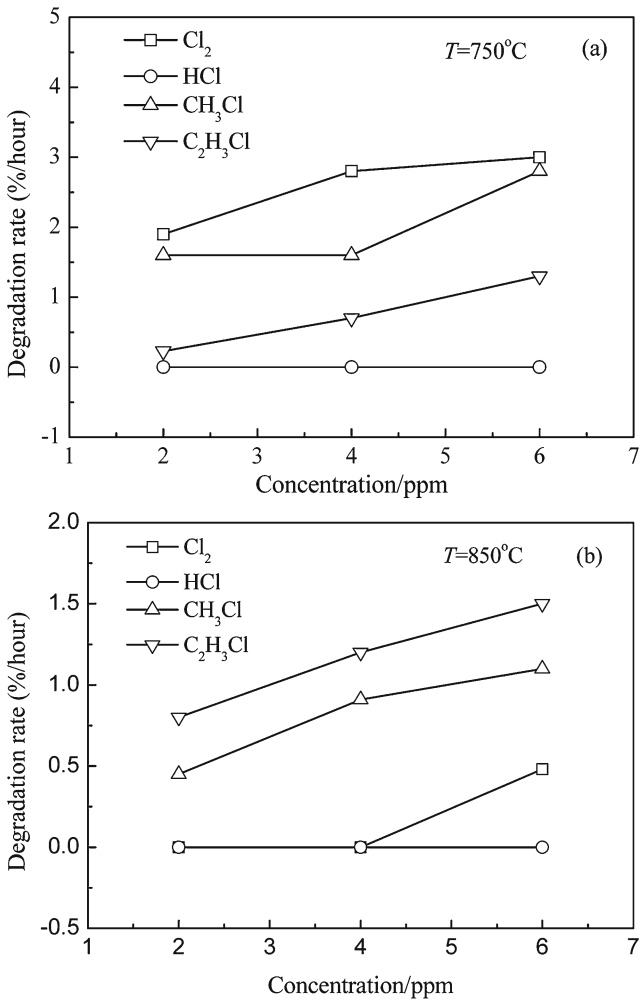

Fig. 7 Degradation rate vs contaminant concentration for the cell poisoning tested at 750 °C **a** and 850 °C **b**

The chemical reactions during poisoning involving $Cl_2(g)$ and HCl(g) can be described by Eqs. 1 and 2. The formation of nickel chloride reduces the anode active area and hinders electrochemical reactions occurred at anode, thus accounting for the degradation due to the addition of $Cl_2(g)$ and

$$Cl_2(g) + Ni(s) \rightleftarrows NiCl_2(s) \quad (1)$$

$$2HCl(g) + Ni(s) \rightleftharpoons NiCl_2(s) + H_2(g) \quad (2)$$

HCl(g). Haga et al. [9] studied the deterioration induced by 5 ppm, 100 ppm and 1,000 ppm $Cl_2(g)$ at 800 °C with a current density of 0.2 $A cm^{-2}$ and attributed the cell performance drop to reaction of Ni and $Cl_2(g)$. However, Trembly et al. [8] ruled out the possibility of nickel chlorine formation by material analyses and thermodynamic calculation. Bao et al. [10] also indicated that nickel chlorine was not stable in reducing environment under SOFC operating conditions. Another possible mechanism of chlorine poisoning is the adsorption of chlorine onto the catalyst nickel surface, which reduces the active region at the anode side and induces the cell performance degradation. The chlorine is formed from Cl molecule decomposition as shown in Eqs. 3 and 4. According to this mechanism,

$$Cl_2(g) \leftrightarrow 2Cl(ad) \quad (3)$$

$$HCl(g) \leftrightarrow Cl(ad) + \frac{1}{2}H_2(g) \quad (4)$$

the degradation in performance can be rapidly recovered since the adsorbed Cl on the nickel surface can be more

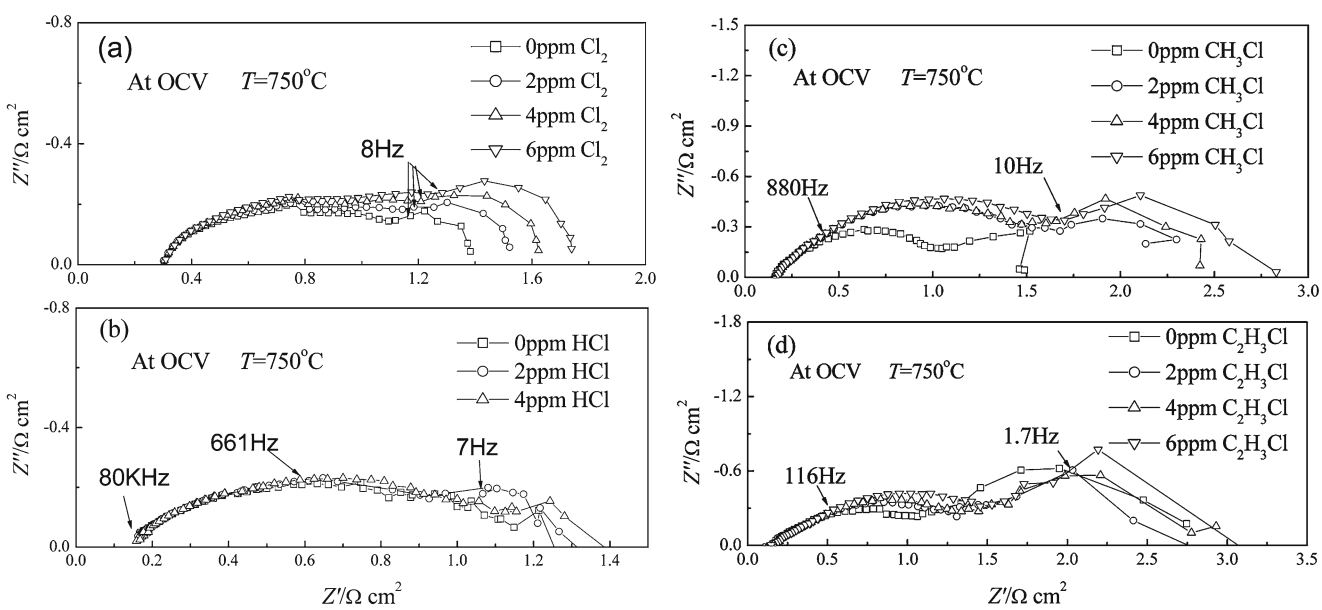

Fig. 8 Nyquist plot of impedance obtained at 750 °C for the cell poisoned by various ppm level contaminants: **a** at Cl_2; **b** HCl; **c** CH_3Cl; **d** C_2H_3Cl

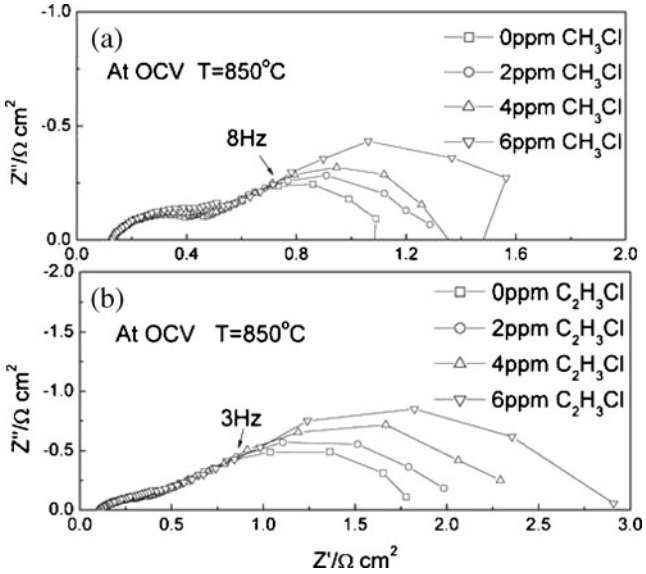

Fig. 9 Impedance spectra recorded at 850 °C with various ppm level of **a** CH_3Cl and **b** C_2H_3Cl

easily converted to stable chlorine specie of HCl(g). This is consistent with the poisoning behavior observed in Figs. 3 and 4. In addition, it has been reported that the most stable chlorine specie under SOFC operation condition is HCl(g) [10], therefore, Eq. 3 is much easier to occur during SOFC operation than Eq. 4. The results that Cl_2(g) can cause degradation to a larger extent than that by HCl(g) under identical conditions is also in accordance with the Cl adsorption mechanism.

As for CH_3Cl(g), its poisoning mechanism can be ascribed to its decomposition into CH_4(g) and HCl(g). Bao et al. [12] reported that CH3Cl(g) could be decomposed into CH_4(g) and HCl(g) under typical SOFC operating environment. However, decomposition of 1 ppm CH_3Cl(g) can only produce 1 ppm HCl(g) according to the decomposition reaction. The present investigation indicates that 1 ppm HCl(g) is unable to induce significant degradation on SOFCs operated at temperatures from 750 and 850 °C, but nevertheless, apparent performance drop is observed by injecting 1 ppm CH_3Cl(g) (Fig. 4). Moreover,

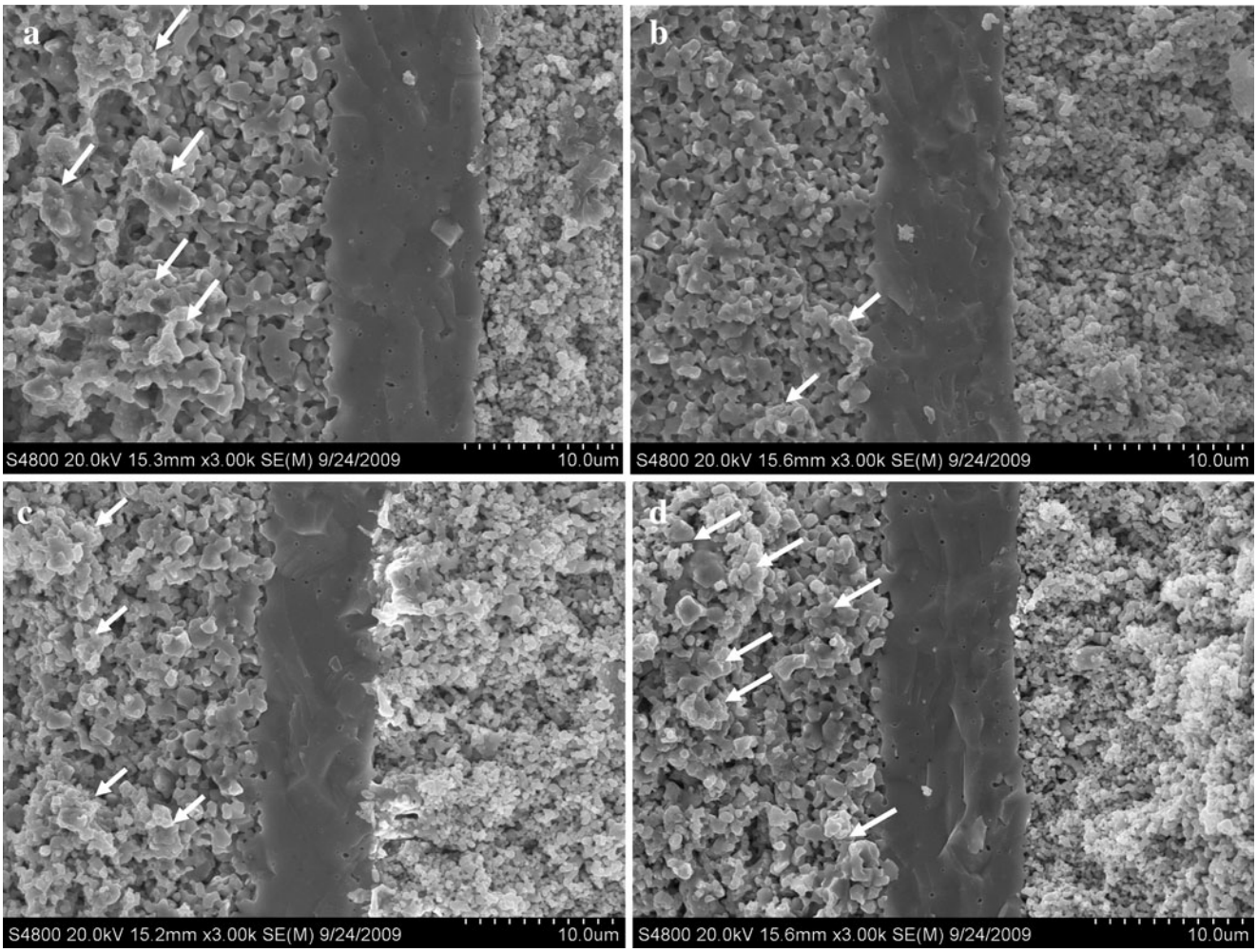

Fig. 10 Cross section of the anode morphology after Cl_2 poisoning **a**; HCl poisoning **b**; CH_3Cl poisoning **c**; C_2H_3Cl poisoning **d**

the equal quantity of HCl(g) cannot cause such poisoning extent degree. Therefore, there should be other mechanism dominating the poisoning effect of CH_3Cl (g). Comparing the poisoning effect for all four Cl contaminants, the poisoning effect of CH_3Cl(g) is similar to that of Cl_2(g). There is a possibility that CH_3Cl(g) poisoning is based on the decomposition of CH_3Cl(g) into CH_4(g) and Cl_2(g).

In order to understand the different poisoning effect of four Cl contaminants, the difference in poisoning extent caused by four contaminants is interpreted in terms of the difference in the unlike binding energy between Cl and methyl or ethyl. All the values of bond energy are presented by report in [20]. The Cl–Cl bonding energy is 243 kJ mol^{-1}, much lower than that of H–Cl bonding energy of 431 kJmol^{-1}, suggesting Cl–Cl can be more readily broken into Cl which can directly deposit on Ni surface and react with Ni to form $NiCl_2$. The bonding energies for CH_3-Cl and C_2H_3-Cl are 356 kJmol^{-1} and 343 kJmol^{-1}, respectively, just lie between the bonding energy of Cl–Cl and Cl–H. This may explain the performance degradation degree caused by CH_3Cl and C_2H_3Cl lies between the degradation degree caused by Cl_2 (higher) and HCl (lower) at 750 °C as shown in Fig. 7a. Although the possibility of CH_3Cl and C_2H_3Cl decomposing into HCl cannot be excluded, this decomposition is a much more difficult process by comparison with the decomposition of Cl from CH_3Cl and C_2H_3Cl because of a higher mean binding energy for H–C (~416 kJmol^{-1}). However, the poisoning degree for the cell exposed to CH_3Cl and C_2H_3Cl at 850 °C as concluded in Fig. 7b is much larger than the cell poisoned by Cl_2. This may be because higher operation temperature facilitates the breakdown of CH_3–Cl and C_2H_3–Cl. The part of methyl "CH_3-" and ethyl "C_2H_3-" may also aggravate the poisoning extent at 850 °C and the degradation caused by these two contaminants appears to be irrecoverable at 850 °C.

Figure 10 shows typical microstructure for the as-poisoned cell. Agglomeration with an average size of 5 μm in diameter can be observed in the anode for the cells poisoned by Cl_2 and C_2H_3Cl as exhibited in Fig. 10a, d, whereas small cluster of particles having an average size of 2~3 μm for the cell exposed to CH_3Cl as displayed in Fig. 10c. For the cell exposed to HCl (Fig. 10b), homogeneous anode microstructure is observed. The different homogeneity in anode microstructure for the cells exposed to different Cl contaminants is in good agreement with the different poisoning degree.

Apparently, the agglomeration exists in the cell subjected to severe poison. This is because the formation of agglomeration reduces contact between nickel particles, resulting in a reducing efficiency of catalyst in anode under SOFC operation conditions. Unfortunately, no chlorine can be detected in neither anode surface, nor anode support layer and active layer using EDS analysis. This limit may be due to the ultra-low contaminant concentrations and the removal of the deposited chloride ($NiCl_2$) by reacting with air to form NiO during cooling [21].

Conclusion

The effect of contaminants containing chlorine in forms of Cl_2(g), HCl(g), CH_3Cl(g), and C_2H_3Cl(g) on the SOFC performance has been investigated at operation temperatures of 750 and 850 °C. Cl_2(g) causes the largest degradation rate at 750 °C and HCl shows the least poisoning effect.

The poisoning effect of CH_3Cl(g) and C_2H_3Cl(g) surpasss the poisoning effect of Cl_2(g) and HCl(g) with the increase of operation temperatures from 750 to 850 °C. EIS analysis indicates Cl contaminants at ppm level can maintain constant *Rs* with increasing concentration but increase *Rp* significantly. Agglomeration in the anode may be the direct effect of Cl contaminant poisoning and the homogeneity of anode microstructure varies with the poisoning effect.

Acknowledgement This work was conducted at Ningbo Institute of Material Technology & Engineering, Chinese Academy of Sciences, and financially supported by the Ningbo Natural Science Foundation (Grant No. 50725101), National 863 Program (No.2007AA05Z140 and No.2009AA05Z122) and China Postdoctoral Science Foundation (20090450745).

References

1. Trembly JP, Gemmena RS, Bayless DJ (2007) The effect of IGFC warm gas cleanup system conditions on the gas—solid partitioning and form of trace species in coal syngas and their interactions with SOFC anodes. J Power Sources 163:986–996
2. EG&G Technical Services, Inc. (2004) Fuel cell handbook, 7th ed. Morgantown, West Virginia
3. Cayan FN, Zhi M, Pakalapati SR, Celik I, Wu N, Gemmen R (2008) Effects of coal syngas impurities on anodes of solid oxide fuel cells. J Power Sources 185:595–602
4. Krishnan GN (2006) Effect of coal contaminants on solid oxide fuel system performance and service life, Technical progress report 2. SRI International, Morgantown
5. Cheng Z, Zha S, Liu M (2007) Influence of cell voltage and current on sulfur poisoning behavior of solid oxide fuel cells. J Power Sources 172:688–693
6. Cheng Z, Liu M (2007) Characterization of sulfur poisoning of Ni-YSZ anodes for solid oxide fuel cells using in situ Raman microspectroscopy. Solid State Ion 178:925–935
7. Rasmussen JFB, Hagen A (2009) The effect of H2S on the performance of Ni-YSZ anodes in solid oxide fuel cells. J Power Sources 191:534–541
8. Trembly JP, Gemmen RS, Bayless DJ (2007) The effect of coal syngas containing HCl on the performance solid oxide fuel cells: investigations into the effect of operational temperature and HCl concentration. J Power Sources 169:347–354
9. Haga K, Adachi S, Shiratori Y, Itoh K, Sasaki K (2008) Poisoning of SOFC anodes by various fuel impurities. Solid State Ion 179:1427–1431

10. Bao J, Krishnan GN, Jayaweera P, Mariano JP, Sanjurjo A (2009) Effect of various coal contaminants on the performance of solid oxide fuel cells: part I. Accelerated testing. J Power Sources 193:607–616
11. Bao J, Krishnan GN, Jayaweera P, Lau KH, Sanjurjo A (2009) Effect of various coal contaminants on the performance of solid oxide fuel cells: part II. ppm and sub-ppm level testing. J Power Sources 193:617–624
12. Bao J, Krishnan GN, Jayaweera P, Sanjurjo A (2010) Impedance study of the synergistic effects of coal contaminants: is Cl a contaminant or a performance stabilizer? J Electrochem Soc 157 (3):B415–B424
13. Li TS, Miao H, Chen T, Wang WG, Xu C (2009) Effect of simulated coal-derived gas composition on H2S poisoning behavior evaluated using a disaggregation scheme. J Electrochem Soc 156:B1383–B1388
14. Li T, Wang WG, Miao H, Chen T, Xu C (2010) Effect of reduction temperature on the electrochemical properties of a Ni/YSZ anode-supported solid oxide fuel cell. J Alloy Compd 495:138–143
15. Haanappel VAC, Mai A, Mertens J (2006) Electrode activation of anode-supported SOFCs with LSM- or LSCF-type cathodes. Solid State Ion 177:2033–2037
16. Wang WG, Guan W, Li H, Wang Z, Wang JX, Wu Y, Zhou S, Zuo G (2009) Solid oxide fuel cell development at NIMTE. ECS Transactions 25(2):85–90
17. Barfod R, Hagen A, Ramousse S, Hendriksen PV, Mogensen M (2006) Breakdown of losses in thin electrolyte SOFCs. Fuel Cells 06(2):141–145
18. Barfod R, Mogensen M, Klemensø T, Hagen A, Liu YL, Hendriksen PV (2007) Detailed characterization of anode-supported SOFCs by impedance spectroscopy. J Electrochem Soc 154:B371–B378
19. Wang WG, Mogensen M (2005) High-performance lanthanum-ferrite-based cathode for SOFC. Solid State Ion 17:6457–6462
20. Speight JG (2005) Perry's standard tables and formulas for chemical engineers. McGraw-Hill, New York, p 29
21. Lussier A, Sofie S, Dvorak J, Idzerda YU (2008) Mechanism for SOFC anode degradation from hydrogen sulfide exposure. Int J Hydrogen Energy 33:3945–3951